Spin resonance in a quantum wire: Anomalous effects of an applied magnetic field

Ar. Abanov,[1] V. L. Pokrovsky,[1,2] W. M. Saslow,[1] and P. Zhou[1]
[1]*Department of Physics and Astronomy, Texas A&M University, College Station, Texas 77843-4242, USA*
[2]*Landau Institute for Theoretical Physics, Chernogolovka, Moscow Distr. 142432, Russia*
(Received 18 April 2011; revised manuscript received 30 January 2012; published 24 February 2012)

We show that in a quantum wire the effective spin-orbit-induced internal magnetic field leads to a narrow spin-flip resonance at low temperatures in the absence of an applied magnetic field. An applied dc magnetic field perpendicular to and small compared with the spin-orbit field enhances the resonance absorption by several orders of magnitude. The component of the applied field parallel to the spin-orbit field separates the resonance frequencies of right and left movers and enables a linearly polarized ac electric field to produce a dynamic magnetization as well as electric and spin currents.

DOI: 10.1103/PhysRevB.85.085311 PACS number(s): 73.21.Hb, 71.70.Ej, 76.20.+q

I. INTRODUCTION

Recently nanodevices have been engineered using materials with predesigned properties.[1–7] This has revitalized interest in comparatively weak electron interactions in nanowires and led to many fascinating discoveries. One of the most important weak interactions is the spin-orbit interaction (SOI). A quantum nanowire with SOI can be formed during growth[3–7] or from a semiconducting film or heterojunction by a proper configuration of the gate electrodes,[8] with a substrate that violates reflection symmetry.

This paper considers electron-spin resonance (ESR) in nanowires with SOI. For ESR in metals an applied magnetic field $\mathbf{B}$ gives distinct Fermi surfaces for up- and down-spins, with the same Zeeman splitting for all electrons. An almost uniform applied ac field of frequency equal to the Zeeman energy then induces sharp transitions between states with the same momentum and opposite spin.

Even a weak SOI changes this picture. It creates an internal "magnetic field" $\mathbf{B}_{\mathrm{SO}}$ that depends linearly on the electron momentum for both Rashba and Dresselhaus SOIs.[9–11] Therefore, for a large enough SOI the ESR is smeared out. As indicated by Shekhter *et al.*,[12] for two-dimensional (2D) systems with only a Rashba interaction, the smearing is comparatively small at temperatures well below the Fermi energy, leading to a narrow ESR—a "chiral resonance." However, Ref. 12 notes that the simultaneous presence of both Rashba and Dresselhaus interactions smears out the resonance since $\mathbf{B}_{\mathrm{SO}}$ and resonance frequency ω_r depend on the 2D momentum direction.

This paper exploits the fact that anisotropic broadening is completely absent for a quantum wire [one-dimensional (1D)], because $\mathbf{B}_{\mathrm{SO}}$ has the same direction for all right-moving particles and the opposite direction for the left movers. Since the Rashba-Dresselhaus SOI is much less than the Fermi energy, the spin-flip energy is well defined. Thus the ESR line is narrow at low temperatures. The spin-flip resonance adsorption in the wire in the absence of an applied magnetic field $\mathbf{B}$ is very weak since it is magnetic dipole induced. The main predictions of this paper are the following:

(i) A component of $\mathbf{B}$ perpendicular to $\mathbf{B}_{\mathrm{SO}}$ activates electric dipole spin-flip transitions and therefore strongly enhances the resonance effects. Typically a $\mathbf{B}$ that is a tenth of $\mathbf{B}_{\mathrm{SO}}$ increases the resonance absorption by four orders of magnitude, while changing ω_r by only 1%.

(ii) The component of $\mathbf{B}$ parallel to $\mathbf{B}_{\mathrm{SO}}$ has little effect on the absorption, but it does separate the resonances of the right and left movers. Linearly polarized resonance radiation then produces a net magnetization and dc electric and spin currents.

The SOI-induced dipole spin-flip excitation in 2D by an ac electric field $\mathbf{E}$ polarized in plane was considered in Ref. 12. Since, because of the SOI, spins in 2D are not collinear the excitation probability is almost independent of $\mathbf{B}$. Previously Rashba and Efros[13] considered a similar problem, but with an ac $\mathbf{E}$ polarized perpendicularly to the plane. To ensure a narrow resonance in this system, $\mathbf{B}$ must significantly exceed $\mathbf{B}_{\mathrm{SO}}$. The authors concluded that a tilted $\mathbf{B}$ is necessary to activate the electric-field–spin interaction. Due to the very high symmetry of their system, their spin-flip probability is proportional to the sixth power of $\mathbf{B}$ (instead of the square, as in the present case). The resulting probability is very small for realistic field values.

This paper is organized as follows: in Sec. II, we present the electronic spectrum and eigenstates with SOI included. We show that there is an energy splitting for electrons with different spin projections. In Sec. III, we consider the effective interaction of the electron spin with an ac electric field, with certain details presented in Appendix A. Section IV discusses the dynamic generation of steady-state currents and magnetization. Relaxation processes are discussed in Sec. V, with certain details given in Appendix B. Numerical estimates are made in Sec. VI. Finally, we present our conclusions in Sec. VII.

II. ELECTRONIC SPECTRUM AND EIGENSTATES

We consider type III-V semiconductors and only their electron bands, to avoid complications associated with degeneracy of the hole band. In p-doped semiconductors, analogous effects of the same order of magnitude should occur for the light holes (with $J = 3/2$ and $J_z = \pm 1/2$, not dissimilar to the present case of $S = 1/2$ and $S_z = \pm 1/2$, where photons can cause transitions between the two states) but not for the heavy holes (with $J = 3/2$ and $J_z = \pm 3/2$, for which photons cannot cause transitions between the two states) or the split-off band (with $J = 1/2$ and $J_z = \pm 1/2$ but with too high an energy of excitation). The 1D electron density n is assumed to be sufficiently high and the temperature sufficiently low to ensure a degenerate Fermi gas. Electron-electron Coulomb

interactions, i.e., Luttinger liquid effects in a 1D electron system,[14,15] will be neglected.[16,17] We also assume that the wire is narrow enough to exclude multiple channels.

In 1D the most general form of the SO interaction, including both Rashba and Dresselhaus terms, is $H_{\rm SO} = (\alpha\sigma_x + \beta\sigma_y)p$, where p is the 1D momentum along the wire direction x[18] and $\boldsymbol{\sigma}$ are the Pauli spin matrices. The total Hamiltonian, without impurity scattering, also includes the kinetic energy $p^2/2m^*$ and the Zeeman term $-\mathbf{b}\boldsymbol{\sigma}$, where $\mathbf{b} = g\mu_B\mathbf{B}/2$ has units of energy. Let us introduce a unit vector $\mathbf{n}$ in the direction $\alpha\hat{x} + \beta\hat{y}$ of $\mathbf{B}_{\rm SO}$ and define the longitudinal and transverse components of the magnetic field: $\mathbf{b} = b_\parallel\mathbf{n} + \mathbf{b}_\perp$. With $\gamma \equiv \sqrt{\alpha^2+\beta^2}$ being the SO velocity, the total Hamiltonian then reads

$$H = p^2/2m^* + (\gamma p - b_\parallel)\mathbf{n}\boldsymbol{\sigma} - \mathbf{b}_\perp\boldsymbol{\sigma}. \tag{1}$$

Its eigenvalues are $E(p,\sigma) = p^2/2m^* + \sigma q$, where $q = \sqrt{(\gamma p - b_\parallel)^2 + \mathbf{b}_\perp^2}$ and $\sigma = \pm 1$ gives the projection of the electron spin along the total effective magnetic field $\mathbf{B}_{\rm e} \equiv \mathbf{B} + \mathbf{B}_{\rm SO}$ and is the eigenvalue of the operator

$$\Sigma = \frac{|\gamma p - b_\parallel|}{q}\left(\mathbf{n} + \frac{\mathbf{b}_\perp}{\gamma p - b_\parallel}\right)\boldsymbol{\sigma}. \tag{2}$$

For a nonzero transverse magnetic field $\mathbf{b}_\perp$, the direction of spin quantization depends on momentum. Figure 1 gives the energy versus magnetic field for small magnetic fields $|\mathbf{b}| \ll p_F^2/2m^*$, with two slightly distorted Rashba parabolas shifted vertically in opposite directions and an avoided crossing (Fig. 1). Here $\mathbf{b}_\parallel$ causes the reflection asymmetry, whereas $\mathbf{b}_\perp$ causes the avoided crossing. The four Fermi momenta correspond to left and right movers and the two values of σ.

For a typical experimental setup the SO velocity $\gamma \ll v_F = p_F/m^*$. If $|\mathbf{b}| \ll \gamma p_F$ then the four Fermi momenta differ only slightly from $\pm p_F = \pm\pi\hbar n/2$ (the Fermi momenta of the wire with $\mathbf{B}_{\rm SO} = \mathbf{B} = \mathbf{0}$) and are given by

$$p_{\sigma\tau} = \tau p_F - \sigma m^*\left[\gamma - \tau\frac{b_\parallel}{p_F} + \frac{\mathbf{b}_\perp^2}{2p_F(\gamma p_F - \tau b_\parallel)}\right], \tag{3}$$

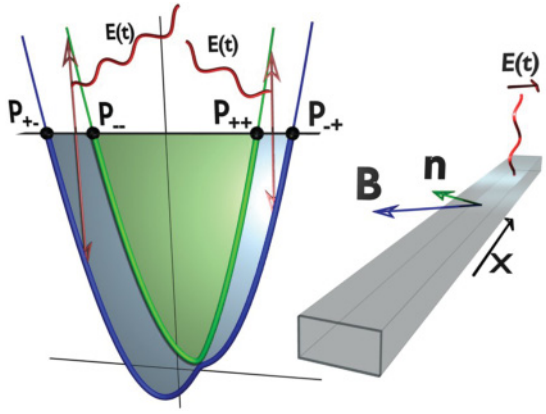

FIG. 1. (Color online) Left: Energy vs momentum is depicted according to Eq. (1). Shadowed regions of the spectrum are occupied. The spin-reversing excitations of the occupied states by the ac electric field are shown. Two transitions are indicated by long vertical arrows. Right: Geometry and directions of the applied magnetic field $\mathbf{B}$ and internal $\mathbf{B}_{\rm SO} \parallel \vec{n}$.

where $\tau = \pm 1$ indicates right (R) and left (L) movers. In the ground state, electrons with spin projection σ fill the momentum interval from $p_{\sigma-}$ to $p_{\sigma+}$.

All states in the interval (p_{--}, p_{++}) are doubly occupied; (p_{+-}, p_{--}) and (p_{++}, p_{-+}) are singly occupied (Fig. 1). A net spin-flip is possible only in the singly occupied intervals (p_{++}, p_{-+}) and (p_{+-}, p_{--}) and requires energy

$$E_{\rm sf} = 2(\gamma|p| - \tau b_\parallel). \tag{4}$$

Thus, for $b_\parallel \neq 0$, there are two different resonance frequencies corresponding to the right and left movers $\tau = \pm 1$. For $\gamma \ll v_F$, the spin-flip energies are centered at $E^0_{\rm sf} = 2(\gamma p_F - \tau b_\parallel)$ and lie in narrow energy bands of intrinsic width Δ, where

$$\Delta = 4m^*\gamma(\gamma - \tau b_\parallel/p_F) = 2\gamma E^0_{\rm sf}/v_F \ll E^0_{\rm sf}. \tag{5}$$

Spin-flip processes can be excited by a resonant applied field with frequency $\omega_r = E^0_{\rm sf}/\hbar$. The temperature must satisfy $T < \hbar\omega_r/k_B$ to avoid thermal smearing.

III. TRANSITION RATE DUE TO LINEARLY POLARIZED AC ELECTRIC FIELD

Let an ac field be linearly polarized along x,

$$\mathbf{E}(t) = \hat{x}E_0(t)e^{-i\omega_0 t} + \hat{x}E_0^*(t)e^{i\omega_0 t}, \tag{6}$$

and have spectral intensity $I(\omega)$ centered about ω_0 with extrinsic width $\Delta\omega \ll \omega_0$. Here $E_0(t)$ is an envelope with frequencies in the interval $\Delta\omega$. Averaged over a time interval t' satisfying $2\pi/\omega_r \ll t' \ll \Delta\omega^{-1}$, the two-time correlator of the field can be represented by an integral: $\overline{E_0^*(t)E_0(t')} = (2\pi)^{-1}\int_{-\infty}^{\infty} I_\omega e^{i\omega(t-t')}d\omega$. $\mathbf{E}$ interacts with the spin since p in the Hamiltonian Eq. (1) must be replaced by $p + \frac{e}{c}A$, where A is the x component of vector potential. We employ the Weyl gauge, where the electric potential $\Phi = 0$, and thus

$$A = -\frac{ic}{\omega_0}[E_0(t)e^{-i\omega_0 t} - E_0^*(t)e^{i\omega_0 t}]. \tag{7}$$

The interaction between the electric field and spin arises from the middle term of Eq. (1) and is given by

$$H_{\rm int} = -\frac{ie\gamma}{\omega_0}[E_0(t)e^{-i\omega_0 t} - E_0^*(t)e^{i\omega_0 t}]\mathbf{n}\boldsymbol{\sigma}. \tag{8}$$

For $\mathbf{b}_\perp = 0$, the interaction Hamiltonian is proportional to the same spin projection $\mathbf{n}\boldsymbol{\sigma}$ that enters Eq. (1), and therefore does not produce spin reversal. Then only magnetic dipole transitions can reverse the spin.[19] Upadhyaya *et al.*[19] note that the SOI makes the magnetization and the internal "magnetic" field depend on the transverse coordinate, which could couple the electric field along y to the spin. We find that to first and second order in the small SOI parameter γ/v_F the contribution of this variation to the electric dipole coupling vanishes. The remaining, third-order, coupling is comparable to or less than the magnetic dipole coupling and can be neglected. (The details of our analysis are given in Appendix A.) This property is specific to 1D systems. In 2D the direction of $\mathbf{B}_{\rm SO}$ changes along with the momentum direction. Thus almost any spin interacts with a linearly polarized electric field. In 1D $\mathbf{b}_\perp \neq 0$ makes electric-field-induced spin reversals not only possible but more probable than magnetic dipole

spin reversals. The matrix element $\langle +|\mathbf{n}\boldsymbol{\sigma}|-\rangle = 2|\mathbf{b}_\perp|/E^0_{\rm sf}$ of the operator $\mathbf{n}\boldsymbol{\sigma}$ produces spin reversal between the two eigenstates of the operator Σ. Time-dependent perturbation theory gives that the spin-flip transition rate for an electron with momentum p is $w = \frac{4e^2\gamma^2}{\hbar^2\omega_0^2}(\mathbf{b}_\perp/E^0_{\rm sf})^2 I_{(2\gamma|p|/\hbar)-\omega_0}$. On resonance, $I_\omega \approx 4\overline{E_0^2}/(\Delta\omega)$, which implies that

$$w \approx 4e^2\overline{E_0^2}\left(\mathbf{b}_\perp/E^0_{\rm sf}\right)^2/p_F^2\Delta\omega. \tag{9}$$

The ratio of the electric and magnetic transition rates is $(c\mathbf{b}_\perp/v_F E^0_{\rm sf})^2$. For InGaAs the ratio c/v_F is about 10^3. Thus, for $b_\perp \sim 10^{-1}E^0_{\rm sf}$ the transition rate Eq. (9) exceeds the magnetic dipole induced rate by four orders, whereas the resonance frequency changes by only 1%.

The perturbation theory used above is valid if the average excited electron occupation number $n_{\rm ex}$ is small, i.e., $w\tau_{\rm eff} \ll 1$, where $\tau_{\rm eff}$ is a characteristic lifetime. In the ballistic regime the time of flight $\tau_f = L/v_F$ plays the role of $\tau_{\rm eff}$. However, if the backscattering time τ_b is much less than τ_f, then diffusion occurs, with lifetime $\tau_{\rm eff} = \tau_f^2/\tau_b \gg \tau_f$. Because saturation occurs for all excitation processes if the recombination rate $w > \tau_{\rm eff}^{-1}$, the probability of excitation is $\min(w\tau_{\rm eff},1)$.

For a narrow spectral width $\Delta\omega$, Rabi oscillations occur. The density of right-moving states subject to spin-resonant excitation is

$$n_{\rm sr} = n\Delta\omega/4\omega_r. \tag{10}$$

IV. DYNAMIC GENERATION OF STEADY-STATE CURRENTS AND MAGNETIZATION

Although we assume that $b_\parallel \ll \gamma p_F$, by Eqs. (4) and (5), if $b_\parallel$ is greater than one-fourth of the linewidth $\Delta \approx 4m^*\gamma^2$, then the resonance frequencies for right and left movers are distinct (with separation $4b_\parallel/\hbar$) and can be excited separately. Thus a resonant linearly polarized ac field can produce a magnetization as well as steady-state electric and spin currents.

Consider a linearly polarized ac field that causes spin flips of right movers, so $n_{\rm ex} = \delta n_{R\uparrow} = -\delta n_{R\downarrow}$. For electrons,

$$n_{\rm ex} = \min(w\tau_{\rm eff},1)n_{\rm sr}, \tag{11}$$

with equal hole density. The spin per electron is $s = n_{\rm ex}/n$. For $w\tau_{\rm eff} < 1$, $n_{\rm ex} = n_{\rm sr}$, so in the ballistic regime

$$j_e = -e(v_{R\uparrow}\delta n_{R\uparrow} + v_{R\downarrow}\delta n_{R\downarrow}) = -2\gamma e n_{\rm ex} = -enw\tau_f\gamma^2/v_F, \tag{12}$$

where $v_{R\downarrow}$ is negative.

To show how diffusion affects the currents, for simplicity we neglect both spin-flip backscattering and energy relaxation but retain backscattering by impurities. Then a simplified set of kinetic equations reads

$$dn^e_{R\uparrow}/dt = wn_{\rm sr} - \left(\tau_{\rm eff}^{-1} + \tau_b^{-1}\right)\delta n^e_{R\uparrow} + \tau_b^{-1}\delta n^e_{L\uparrow}, \tag{13}$$

$$dn^e_{L\uparrow}/dt = -\left(\tau_{\rm eff}^{-1} + \tau_b^{-1}\right)\delta n^e_{L\uparrow} + \tau_b^{-1}\delta n^e_{R\uparrow}. \tag{14}$$

The ac field creates equal numbers of electrons and holes with parallel spins, and this property is maintained by the backscattering if spin-flip processes are negligible. The pumped spin is polarized approximately along $\mathbf{n} + \mathbf{b}_\perp/\gamma p_F$. Its steady-state absolute value per unit length is $s_{\rm eff} = w\tau_{\rm eff}n_{\rm sr}$. The spin current j_s is $j_s = g\mu_B v_F wn_{\rm sr}\tau_{\rm eff}\tau_b/(2\tau_{\rm eff} + \tau_b)$, and j_e is

$$j_e = -2e\gamma wn_{\rm sr}\frac{\tau_{\rm eff}\tau_b}{2\tau_{\rm eff} + \tau_b} + ewn_{\rm sr}\frac{b_\perp^2\tau_{\rm eff}(4\tau_{\rm eff} + \tau_b)}{\gamma p_F^2(2\tau_{\rm eff} + \tau_b)}. \tag{15}$$

Equation (15) shows that the electric current changes sign in the diffusive regime at $b_\perp > \gamma p_F\sqrt{\tau_b/2\tau_{\rm eff}}$. This happens because backscattering equalizes the number of left- and right-moving excitations, whose velocities differ. For resonance of left movers, at frequency $\omega_r^L = 2(\gamma p_F + b_\parallel)/\hbar$, the magnetization and currents are reversed.

The generation of currents by an ac field is similar to the photogalvanic effect predicted by Ivchenko and Pikus[20] and by Belinicher.[21] More recently many clever modifications of this effect have been proposed and experimentally observed.[22–24] They are mostly realized in 2D systems, but more importantly, unlike 1D, *nonresonant* optical or infrared radiation is used. In most cases, dynamic magnetization and electric current generation require a circularly polarized pumping field, whereas for a quantum wire in $\mathbf{B} \neq \mathbf{0}$ the same effect can be produced by a linearly polarized source. The 1D geometry implies a strong dependence of the resonance line and transition probability on $\mathbf{B}$.

V. RELAXATION PROCESSES

At low temperature the main mechanism for electron energy relaxation is phonon emission. If the corresponding relaxation time $\tau_{\rm ep}$ becomes comparable to or less than τ_f, energy relaxation occurs before electrons and holes leave the wire. The total spin is not changed but the excitation velocities may decrease because lower energy means lower p and lower v. On the other hand, energy relaxation removes particles from the excited states and fills the depleted states. This makes an increase of power in the applied ac field more effective.

The electron-phonon interaction is modeled by a standard Hamiltonian $H_{\rm ep} = U\int \nabla\mathbf{u}(\mathbf{x})\psi^\dagger(\mathbf{x})\psi(\mathbf{x})$, where $\mathbf{u}(\mathbf{x})$ is the displacement vector, $\psi(\mathbf{x})$ is the electron field operator, and U is the deformation potential. Electrons in the wire are always 1D, but phonons can be 1D, 2D, or three-dimensional (3D) depending on the experimental setup. Let M and a be the lattice cell mass and lattice constant, and let u be the sound velocity. Then, for an electron with momentum deviating by ξ from the Fermi point and emitting 3D phonons, the relaxation rate is

$$\tau_{\rm ep}^{-1} = \frac{U^2}{6\pi\hbar Muv_F}\left(\frac{v_F\xi a}{u\hbar}\right)^3. \tag{16}$$

The detailed calculation is given in Appendix B.

In 2D and 3D systems elastic scattering (diffusion) leads to spin relaxation by the Dyakonov-Perel mechanism,[25,26] because the direction of $\mathbf{B}_{\rm SO}$ depends on the direction of the $\mathbf{p}$ and is randomized by diffusion. In 1D for $\mathbf{b}_\perp = 0$ the direction of $\mathbf{B}_{\rm SO}$ is the same for all electrons, so the Dyakonov-Perel mechanism does not apply. A suppression of Dyakonov-Perel relaxation in 1D was found in numerical calculations.[27] However, for $\mathbf{b}_\perp \neq 0$, spin flip does occur in backscattering, but its probability is of the order of $(\mathbf{b}_\perp/E^0_{\rm sf})^2$

and can be neglected. Other spin-relaxation mechanisms, such as phonon emission combined with SOI, are much weaker.

VI. NUMERICAL ESTIMATES

All numerical estimates are for $In_{0.53}Ga_{0.47}As$. We take $m^* = 4.3 \times 10^{-29}$ g $\approx 0.05 m_e$, $\alpha = 1.08 \times 10^6$ cm/s, and $g = -0.5$.[28–30] A typical 2D electron density is 2×10^{12} cm^{-2}. Take wire thickness $a = 5$ nm and width $d = 10$ nm. Then we find 1D density $n = 10^6$ cm^{-1}, $p_F = 1.65 \times 10^{-21} g$ cm/s, and $v_F = 0.38 \times 10^8$ cm/s. Assuming $\alpha = \beta$, we have $\omega_r = 4.8 \times 10^{12}$ s^{-1} ($\sim$0.8 THz) and intrinsic width $\delta = \Delta/\hbar \approx 3.8 \times 10^{11}$ s^{-1}. The value $\overline{E_0^2}$ in Eq. (9) is determined by the source power in the terahertz range. Although standard cascade lasers have power in the range 1 mW to 1 W,[31,32] the power can be strongly enhanced by nonlinear devices, and in very short pulses (1 ps) it can reach 1 MW.[33–36] The free-electron laser at University of California, Santa Barbara, provides a continuous power of 1–6 kW for the frequency range 0.9–4.75 THz. On focusing, the energy flux rises to 40 kW/cm^2.[36] For the moderate flux $S = 1$ kW/cm^2, we find $\overline{E_0^2} = 4\pi S/c = 4.19$ ergs cm^{-3}. For $B_\perp = 10$ T we have $b_\perp/E_{\rm sf}^0 = 0.05$, and Eq. (9) yields $w = 0.92 \times 10^{10}$ s^{-1}. As noted above, w can be increased by changing the power or the focus area. For length $L = 1$–$10\,\mu$m the time of flight is $\tau_f = 2.6 \times (10^{-12}$–$10^{-11})$ s. The backscattering time τ_b can be estimated from typical mobilities $\mu = e\tau/m^* = (2 \times 10^4$–$4 \times 10^5)$ cm^2/V s in the bulk or film.[37] Since the scattering cross-section area is much less than the wire cross-section area, τ can be identified with τ_b. Typical values are $\tau_b = 5 \times 10^{-13}$–$10^{-11}$ s. In this case the regime is either diffusive or marginally diffusive-ballistic.

First consider a ballistic regime with $\tau_f = 1.1 \times 10^{-11}$ s. By Eq. (12) the electric current equals 1 nA. The ratio of the spin current to the electric current in units of elementary charges per second is $v_f/(2\gamma) \approx 12$. The magnetization per electron, in Bohr magnetons, is $\frac{n_{\rm st}}{n} w\tau_{\rm eff} \sim 0.004$. Now consider a diffusive regime with $\tau_b = 1.1 \times 10^{-12}$ s and $\tau_f = 1.1 \times 10^{-11}$ s, so $\tau_{\rm eff} = 1.1 \times 10^{-10}$ s. By Eq. (15) the electric current is $I = j_e = 0.12$ nA and the magnetization per electron is $0.02\mu_B$. The temperature must be maintained below $2\gamma p_F/k_B \approx 35$ K. $w\tau_{\rm eff}$ in this case is approximately one, indicating that saturation has been attained. For energy relaxation we assume 3D phonons. For InGaAs we take $U = 16$ eV, $u = 3.3 \times 10^5$ cm/s,[38] $a = 5$ Å, $M = 1.8 \times 10^{-22}$ g, and $\xi = m^*\gamma$. Then by Eq. (8) $\tau_{\rm ep} = 1.4 \times 10^{-12}$ s. With 2D and 1D phonons the formulas differ, but numerical estimates give the same order of magnitude. This result shows that, even in the ballistic regime, $\tau_{\rm ep}$ is usually much shorter than τ_f, so energy relaxation is substantial, which decreases the currents.

VII. CONCLUSIONS

In a 1D degenerate Fermi gas the SOI gives rise to a spin resonance. We predict that in one dimension this resonance is extremely sensitive to the component of the applied magnetic field perpendicular to the internal $\mathbf{B}_{\rm SO}$. The resonance frequency is typically in the terahertz region with relative width depending linearly on the Dresselhaus and Rashba SO constants. The applied longitudinal magnetic field (parallel to the internal SO field) separates the resonance frequencies of the left and right movers, producing charge and spin currents. A nonzero component of the applied magnetic field $\mathbf{B}$ perpendicular to $\mathbf{B}_{\rm SO}$ couples an ac electric field to the spin, providing a very efficient spin-flip mechanism. Otherwise, electron spin is flipped only by the weak magnetic dipole interaction. On resonance an ac electric field linearly polarized along the wire produces a steady-state charge current, spin current, and magnetization. These effects can be easily controlled by the static applied magnetic field and the gate voltage.

ACKNOWLEDGMENTS

We thank A. M. Finkelstein and M. Khodas for theoretical discussions and J. Kono for discussing the experimental situation. This work was supported by the Department of Energy under Grant No. DE-FG02-06ER46278. Ar. A. was supported by Grant No. NSF0757992 and Welch Foundation Grant No. A-1678.

APPENDIX A

In this Appendix we present the calculation, referred to in Sec. III, of the matrix element responsible for the spin flipping due to coupling to the transverse electric field. We treat the spin-orbit interaction as a perturbation and show that the matrix element is zero to first and second order in the SOI coupling constants α and β. The first nonzero contribution comes in the third order in spin-orbit interaction. We start from the same Hamiltonian as before. We introduce the frame of reference with the x axis along the wire and y axis along the wide side of the cross section whose linear size is denoted as W. Because we are only interested in the linear coupling to the y component of the electric field, we take A_x, A_z, and the magnetic field B to be zero. Then the Hamiltonian, up to linear terms in the ac field, reads

$$H = H_{\rm kin} + H_{\rm so} + H_{\rm ac}, \tag{A1}$$

where

$$H_{\rm kin} = \frac{p_x^2 + p_y^2}{2m^*}, \tag{A2}$$

$$H_{\rm so} = p_x(\alpha\sigma_x + \beta\sigma_y) - p_y(\alpha\sigma_y + \beta\sigma_x), \tag{A3}$$

$$H_{\rm ac} = \frac{e}{c} A_y v_y. \tag{A4}$$

Here $v_y = \frac{p_y}{m^*} - (\beta\sigma_x + \alpha\sigma_y)$ and we assume that the effective mass m^* is the same in both x and y directions. Let us represent the Hamiltonian Eq. (A1) without the last term as $H = H_0 + V$, where $H_0 = H_{\rm kin} + p_x(\alpha\sigma_x + \beta\sigma_y)$ and the perturbation is $V = -p_y(\alpha\sigma_y + \beta\sigma_x)$. The stationary states $|n, p_x, \tau\rangle_0$ of the Hamiltonian H_0 are direct products of the eigenstates of p_x, p_y^2 and the spin operator $\tau_z = (\alpha\sigma_x + \beta\sigma_y)/\gamma$. The corresponding wave functions are

$$\psi^{(0)}_{n,p_x,\tau} = f_n(y) e^{ip_x x} \chi_\tau. \tag{A5}$$

Here $f_n(y)$ is the transverse part of the wave function, and χ_τ is an eigenspinor of τ_z with the eigenvalue $\tau = \pm 1$. The energy of the state $|n, p_x, \tau\rangle_0$ is $E^0_{n,p_x,\tau} = E^0_{n,p_x} + \gamma p_F$, where $E^0_{n,p_x} = {}_0\langle n, p_x, \tau | H_{\rm kin} | n, p_x, \tau\rangle_0$. The first-order perturbation-

theory correction τ to the wave function Eq. (A5) is

$$\psi^{(1)}_{n,p_x,\tau} = -\sum_{m\neq n,\tau'} |m,p_x,\tau'\rangle_0 \times \frac{{}_0\langle m,p_x,\tau'|(\alpha\sigma_y+\beta\sigma_x)p_y|n,p_x,\tau\rangle_0}{E^0_{n,p_x}-E^0_{m,p_x}}, \quad \text{(A6)}$$

where we neglect the contribution of the first SOI term $p_x(\alpha\sigma_x+\beta\sigma_y)$ to the energies in the denominator, retaining the leading term $E^0_{n,p_x}-E^0_{m,p_x}$. In order to calculate the sum in Eq. (A6) we note that in the zeroth-order approximation $p_y = \frac{im^*}{\hbar}[H_{\rm kin},y]$. Then this equation can be simplified to read

$$\psi^{(1)}_{n,p_x,\tau} = \frac{im^*}{\hbar}\sum m\neq n,\tau'|m,p_x,\tau'\rangle_0 \times {}_0\langle m,p_x,\tau'|(\alpha\sigma_y+\beta\sigma_x)y|n,p_x,\tau\rangle_0. \quad \text{(A7)}$$

Finally, by choosing the frame of coordinates so that $\langle n|y|n\rangle = 0$ and using the completeness relation $\sum_{m,\tau'}|m,p_x,\tau'\rangle_0 {}_0\langle m,p_x,\tau'| = I$, we find the first-order correction to the eigenstate $|n,p_x,\tau\rangle_0$:

$$|n,p_x,\tau\rangle_1 = \frac{im^*}{\hbar}(\alpha\sigma_y+\beta\sigma_x)y|n,p_x,\tau\rangle_0. \quad \text{(A8)}$$

Now we consider the effect of the transverse ac electric field. We are interested in the off-diagonal term of the operator $\frac{e}{c}A_y\upsilon_y$ for the states of a fixed band, i.e., in the matrix element

$$\frac{e}{c}A_y\langle n,p_x,-|\upsilon_y|n,p_x,+\rangle, \quad \text{(A9)}$$

where $+$ and $-$ represent the up and down eigenstates for the spin operator τ_z, respectively. Again employing the Heisenberg equation $\upsilon_y = \frac{i}{\hbar}[H_{\rm kin}+H_{\rm so},y]$, one can transform the matrix element Eq. (A9) as follows:

$$\langle n,p_x,-|\,\upsilon_y\,|n,p_x,+\rangle = \frac{i}{\hbar}(E_{n,p_x,-}-E_{n,p_x,+})\,\langle n,p_x,-|\,y\,|n,p_x,+\rangle\,. \quad \text{(A10)}$$

The energies belonging to a fixed band n and different spin projections differ only because of the SOI. Therefore, an expansion of the difference $E_{n,p_x,-}-E_{n,p_x,+}$ in terms of SOI coupling constants begins with a linear term of α and β:

$$E_{n,p_x,-}-E_{n,p_x,+}\approx -2\gamma p_x. \quad \text{(A11)}$$

Thus, to obtain the contribution to the matrix element Eq. (A10) linear in the SOI coupling constants, it is necessary to calculate the matrix element of y with the zeroth-order wave function $|n,p_x,\tau\rangle_0\,(\tau=\pm)$, for which the space and spin variables are factored. Therefore, the matrix element of y contains the scalar product $\langle-|+\rangle$, which equals zero. To find the matrix element in Eq. (A10) to the second order in α and β, we need to use $|n,p_x,\tau\rangle_1$ for the matrix element of y. Then, using Eq. (A8), one finds

$${}_1\langle n,p_x,-|y|n,p_x,+\rangle_0 + {}_0\langle n,p_x,-|y|n,p_x,+\rangle_1 = \frac{im^*}{\hbar}{}_0\langle n,p_x,-|(\alpha\sigma_y+\beta\sigma_x)[y,y]|n,p_x,+\rangle_0. \quad \text{(A12)}$$

Since this matrix element is zero, the y component of the electric field produces no spin-flip processes in the second order in α and β as well.

The quickest way to calculate the Hamiltonian $H_{\rm ac}$ in the third order or, equivalently, the matrix element of y in the second order goes through a unitary transformation $U=e^F$, where $F=-i\frac{m^*}{\hbar}y(\alpha\sigma_y+\beta\sigma_x)$. Applying it to the Hamiltonian (without the ac field term), and truncating the Baker-Hausdorff series at the second order in α and β (recall that $\gamma=\sqrt{\alpha^2+\beta^2}$), we find

$$H_U = U(H_{\rm kin}+H_{\rm so})U^{-1}\approx H+[F,H] = H_0+V_U+\text{const}, \quad \text{(A13)}$$

where

$$H_0 = \frac{p_x^2+p_y^2}{2m^*}+p_x\gamma\tau_z \quad \text{(A14)}$$

is the starting approximation Hamiltonian introduced earlier, and

$$V_U = \frac{2m^*}{\hbar}(\beta^2-\alpha^2)yp_x\sigma_z \quad \text{(A15)}$$

is the transformed perturbation that is proportional to squares of the SOI constants. Note that the transformed eigenstate $|n,p_x,\tau\rangle_U$ obeys the same boundary conditions as the initial one. Thus, the transformed state $|n,p_x,\tau\rangle_U$ differs from the zero approximation state $|n,p_x,\tau\rangle_0$ by the second-order correction:

$$|n,p_x,\tau\rangle_{U,2} = \frac{2m^*p_x}{\hbar}(\beta^2-\alpha^2)\sum_{m\neq n,\tau'}|m,p_x,\tau'\rangle_0 \times {}_0\langle m,p_x,\tau'|y\sigma_z|n,p_x,\tau\rangle_0 \times \frac{1}{E^0_{n,p_x}-E^0_{m,p_x}}. \quad \text{(A16)}$$

The state vector we are looking for, $|n,p_x,\tau\rangle = U^{-1}|n,p_x,\tau\rangle_U$, has an additional term of the second order equal to the operator $F^2/2$ acting on the zeroth-order state. Since F^2 is proportional to the unit operator, it does not contribute to the matrix element in Eq. (A10). With Eqs. (A5), (A10), (A11), and (A16), we obtain the matrix element to the third order in α and β:

$$\langle n,p_x,-|\,\upsilon_y\,|n,p_x,+\rangle = -\sum_{m\neq n}\frac{i}{\hbar}\frac{8m^*p_x^2}{\hbar}\gamma(\beta^2-\alpha^2)\frac{|{}_0\langle m,p_x|y|n,p_x\rangle_0|^2}{E^0_{n,p_x}-E^0_{m,p_x}}, \quad \text{(A17)}$$

where we use matrix elements for the spin operator σ_z between the eigenstates of the operator τ_z $\langle\pm|\,\sigma_z\,|\pm\rangle = 0$ and $\langle\mp|\,\sigma_z\,|\pm\rangle = 1$. The zeroth-order off-diagonal matrix element reads

$${}_0\,\langle m,p_x|\,y\,|n,p_x\rangle_0 = -\frac{8nmW\sin\left(\frac{m+n}{2}\pi\right)}{\pi^2(m^2-n^2)^2} \quad \text{(A18)}$$

and

$$E^0_{n,p_x}-E^0_{m,p_x} = \frac{\hbar^2\pi^2(n^2-m^2)}{2m^*W^2}. \quad \text{(A19)}$$

Thus, the matrix element of the velocity υ_y from Eq. (A10) can be expressed in terms of an infinite series:

$$\langle n,p_x,-|\,\upsilon_y\,|n,p_x,+\rangle = i(\beta^2-\alpha^2)\gamma\frac{1024m^{*2}W^4p_x^2n^2}{\hbar^4\pi^6} \times\sum_{m=n+\text{odd}}\frac{m^2}{(m^2-n^2)^5}. \tag{A20}$$

For $n=1$ the sum is $\sum_{k=1}^{\infty}\frac{4k^2}{(4k^2-1)^5}=\frac{\pi^2(15-\pi^2)}{3072}\approx 0.016\,48$. We can now obtain the coefficient at $e/cA_y\upsilon_y$ for the spin-flip amplitude induced by the transverse electric field; it is given by

$$i\gamma\frac{m^{*2}W^4p_x^2(\beta^2-\alpha^2)}{\hbar^4}\times 0.0176. \tag{A21}$$

If we let $W=10$ nm, $p_F=1.65\times10^{-21}g$ cm/s, $\alpha=1.08\times10^6$ cm/s, and $\upsilon_F=0.38\times10^8$ cm/s, then we find that the upper bound for the coefficient of γ, given by Eq. (A21), is $\sim10^{-5}$. It is five decimal orders less than the similar coefficient of $(e/c)A_x\tau_z$. However, the latter does not produce a spin-flip transition. The transverse magnetic field makes spin flips possible but decreases the coefficient by a factor $(\frac{b_\perp}{\gamma p_F})^2\approx 0.01$. Nevertheless the anisotropy ratio of the amplitudes is about 0.001. The anisotropy of the spin-flip probability is about 10^{-6}. Thus, resonant excitation by an ac electric field polarized along the y axis is very ineffective and practically unobservable. However, the amplitude Eq. (A21) depends very strongly on W. Therefore, the width cannot be increased significantly (it can be increased by no more than a factor of three). On the other hand, a significant change of W would violate the condition of one channel.

APPENDIX B

In this Appendix we derive the electron-phonon relaxation time τ_{ep}. As noted in Sec. V, the standard Hamiltonian for the electron-phonon interaction is

$$H_{\text{ep}}=U\int\nabla\mathbf{u}(\mathbf{r})\psi^\dagger(\mathbf{r})\psi(\mathbf{r})d^3r, \tag{B1}$$

where $\mathbf{u}(\mathbf{r})$ (the displacement vector) and $\psi(\mathbf{r})$ (the electron field operator) are given by the formulas

$$\mathbf{u}(\mathbf{r})=\sum_{\mathbf{q}}\sqrt{\frac{\hbar}{2NM\omega_{\mathbf{q}}}}(b_{\mathbf{q}}e^{i\mathbf{q}\cdot\mathbf{r}}+b_{\mathbf{q}}^\dagger e^{-i\mathbf{q}\cdot\mathbf{r}})\mathbf{e}_{\mathbf{q}}, \tag{B2}$$

$$\psi(\mathbf{r})=\frac{2}{\sqrt{L_xL_yL_z}}\sum_k a_k e^{ikx}\sin\frac{\pi y}{L_y}\sin\frac{\pi z}{L_z}. \tag{B3}$$

Here N is the number of elementary cells in the crystal supporting the phonons (in the 1D case it coincides with the wire); M is the mass of the elementary cell; L_x, L_y, and L_z are the linear sizes of the quantum wire in the x, y, and z directions; a_k is the annihilation operator for an electron with wave vector k; $b_{\mathbf{q}}$ ($b_{\mathbf{q}}^\dagger$) is the annihilation (creation) operator for a phonon with wave vector $\mathbf{q}$; $\omega_{\mathbf{q}}=uq$ is the phonon frequency; u is the sound velocity; and $\mathbf{e}_{\mathbf{q}}$ is the unit polarization vector of the sound vibration.

We consider in some detail the case of 3D phonons and denote the components of $\mathbf{q}$ by q_x, q_y, and q_z. Putting $\mathbf{u}(\mathbf{r})$ and $\psi(\mathbf{r})$ defined by Eqs. (B2) and (B3) into H_{ep} and integrating over the coordinates within the wire, one arrives at the following electron-phonon Hamiltonian in momentum space:

$$H_{\text{ep}}=\sum_{k,\mathbf{q}}\sqrt{\frac{\hbar U^2}{2NM\omega_{\mathbf{q}}}}f(q_yL_y)f(q_zL_z)(\mathbf{e}_{\mathbf{q}}\cdot\mathbf{q}) \times(b_{\mathbf{q}}+b_{-\mathbf{q}}^\dagger)a_{k+q_x}^\dagger a_k, \tag{B4}$$

where $f(x)=\frac{2\sin(x/2)}{x(x^2/4\pi^2-1)}$. At a very low temperature the number of thermal excitations is small and can be neglected, and dominantly the phonon emission due to the Cherenkov effect leads to energy relaxation. In this process an electron with momentum p above the Fermi momentum p_{F++} emits a phonon with momentum $\mathbf{q}$ and turns into an electron with momentum $p-\hbar q_x$. The probability of this process per unit time in first-order perturbation theory is

$$w_{\text{ep}}(p,\mathbf{q})=\frac{\pi U^2q}{NMu}f^2(q_yL_y)f^2(q_zL_z)\delta(E_{p-\hbar q_x}+\hbar\omega_{\mathbf{q}}-E_p). \tag{B5}$$

The additional assumption that $q_yL_y\ll1, q_zL_z\ll1$ reduces the functions $f(q_yL_y)$ and $f(q_zL_z)$ to one. Let the electron in the initial state be a right mover with spin up (left movers can be considered similarly). In the phonon emission process the spin projection is conserved except for terms of order $(\frac{b_\perp}{\gamma p_F})^2$. In the final state the electron can either remain a right mover or become a left mover. The corresponding probabilities per unit time are denoted by Γ_{RR} and Γ_{RL}. In first-order perturbation theory both can be expressed formally by the same integral:

$$\Gamma_{RR,RL}=\frac{U^2a^3}{8\pi^2Mu}\int q\delta(E_{p-\hbar q_x}+\hbar\omega_{\mathbf{q}}-E_p), \tag{B6}$$

where we have used the relation $N=V_s/a^3$ with V_s being the volume of the substrate and a its lattice constant. The difference between Γ_{RR} and Γ_{RL} is due to different integration regions, determined by the energy- and momentum-conservation laws. For the RR process with the initial electron momentum $p_{++}+\xi$ the integration over q_x proceeds in the interval $0\leqslant\hbar q_x\leqslant\xi$. In the RL process the value $\hbar q_x$ is close to $2p_F$. Considering first the RR process, we find from energy conservation that q obeys the relationship $q\approx(\upsilon_F/u)q_x$. With this relation the integration becomes straightforward, resulting in

$$\Gamma_{RR}=\frac{U^2}{12\hbar\pi Mu\upsilon_F}\left(\frac{\upsilon_F\xi a}{\hbar u}\right)^3. \tag{B7}$$

For the RL process, conservation of energy can be satisfied only for $\xi\geqslant2m^*u$. For lower energies this process does not contribute to the relaxation rate. The interval of integration over q_x well above the threshold is $2p_F+\xi<\hbar q_x<2p_F+2\xi$. It is convenient to introduce a new variable, $\kappa=2p_F+2\xi-\hbar q_x$, varying in the interval $(0,\xi)$. In the same approximation, conservation of energy implies $\hbar q\approx(\upsilon_F/u)\kappa$. After these simplifications the calculation of Γ_{RL} becomes elementary, resulting in $\Gamma_{RL}=\Gamma_{RR}$. Thus in total the relaxation probability for electrons due to the electron-phonon interaction is given by Eq. (16).

For 2D phonons, similar calculations give the following result for $\xi \gg 2m^*u$:

$$\left.\frac{1}{\tau_{\rm ep}}\right|_{\rm 2D} = \frac{U^2 a^3 v_F \xi^2}{2\hbar^3 u^3 \pi d M}, \tag{B8}$$

where d is the thickness of the film.

For a velocity v_F much larger than the sound velocity u, from the energy- and momentum-conservation laws we know that forward scattering is impossible, so only backscattering with $\hbar q \approx 2p_F$ can occur. Following the same derivation as above, we obtain the relaxation probability for 1D phonons as

$$\left.\frac{1}{\tau_{\rm ep}}\right|_{\rm 1D} \approx \frac{U^2 m^* a^3}{\hbar^2 A M u}, \tag{B9}$$

where A is the area of the y-z surface of the substrate. The relaxation time for 2D phonons at $d \approx 10$ nm has the same order of magnitude as for 3D phonons. For 1D phonons, if $A = 100\ \text{nm}^2$ then $\tau_{\rm ep}$ is about 300 times longer.

[1] Y. Wu, J. Xiang, C. Yang, W. Lu, and C. M. Lieber, Nature (London) **430**, 61 (2004).

[2] L. J. Lauhon, M. S. Gudiksen, and C. M. Lieber, Physical and Engineering Sciences **362**, 1247 (2004).

[3] S. B. Kim, J. R. Ro, K. W. Park, and E. H. Lee, J. Cryst. Growth **201**, 828 (1999).

[4] O. Zsebok, J. V. Thordson, B. Nilsson, and T. G. Andersson, Nanotechnology **12**, 32 (2001).

[5] C. L. Zhang, Z. G. Wang, Y. H. Chen, C. X. Cui, B. Xu, P. Jin, and R. Y. Li, Nanotechnology **16**, 1379 (2005).

[6] J. H. Dai, Y. L. Lin, S. C. Lee, S. Y. Lin, and J. Y. Chi, in *5th IEEE Conference on Nanotechnology*, Vol. 1, pp. 407–409 (2005).

[7] M. A. Verheijen, G. Immink, T. D. Smet, M. T. Borgstrom, and E. P. A. M. Bakkers, J. Am. Chem. Soc. **128**, 1353 (2006).

[8] T. Schapers, J. Knobbe, and V. A. Guzenko, Phys. Rev. B **69**, 235323 (2004).

[9] G. Dresselhaus, Phys. Rev. **100**, 580 (1955).

[10] E. I. Rashba, Sov. Phys. Solid State **2**, 1109 (1960).

[11] Y. A. Bychkov and E. I. Rashba, JETP Lett. **39**, 78 (1984).

[12] A. Shekhter, M. Khodas, and A. M. Finkelstein, Phys. Rev. B **71**, 165329 (2005).

[13] E. I. Rashba and A. L. Efros, Phys. Rev. Lett. **91**, 126405 (2003).

[14] W. Hausler, Phys. Rev. B **63**, 121310 (2001).

[15] M. Governale and U. Zulicke, Solid State Commun. **131**, 581 (2004).

[16] In the Luttinger liquid picture the same resonance is described as excitation of a spin wave. Preliminary calculations show that the interaction renormalizes the speed of spin-wave propagation but does not provide a finite linewidth, which occurs only due to the deviation of the fermion dispersion from linearity.

[17] M. Khodas, M. Pustilnik, A. Kamenev, and L. I. Glazman, Phys. Rev. B **76**, 155402 (2007).

[18] p_y and p_z are neglected as the transverse motion is quantized, so $\mathbf{B}_{\rm SO} = (\alpha p, \beta p, 0)$.

[19] P. Upadhyaya, S. Pramanik, S. Bandyopadhyay, and M. Cahay, Phys. Rev. B **77**, 045306 (2008).

[20] E. I. Ivchenko and G. E. Pikus, Sov. Phys. JETP Lett. **27**, 604 (1978).

[21] V. Belinicher, Phys. Lett. A **66**, 213 (1978).

[22] S. Ganichev and W. Prettl, J. Phys. Condens. Matter **15**, R935 (2003).

[23] S. Tarasenko and E. Ivchenko, JETP Lett. **81**, 231 (2005).

[24] S. D. Ganichev, S. N. Danilov, V. V. Belkov, S. Giglberger, S. A. Tarasenko, E. L. Ivchenko, D. Weiss, W. Jantsch, F. Schaffler, D. Gruber, and W. Prettl, Phys. Rev. B **75**, 155317 (2007).

[25] M. I. Dyakonov and V. I. Perel, Sov. Phys. JETP **33**, 1053 (1971).

[26] M. I. Dyakonov, "Basics of Semiconductor and Spin Physics," Chapter 1 in *Spin Physics in Semiconductors* (Springer, New York, 2008).

[27] A. A. Kiselev and K. W. Kim, Phys. Rev. B **61**, 13115 (2000).

[28] For simplicity we neglect the anisotropy of the g factor. Experimentally it is not small and must be accounted for in a more accurate theory.

[29] M. V. Dorokhin, Y. A. Danilov, P. B. Demina, V. D. Kulakovskii, O. V. Vikhrova, S. V. Zaitsev, and B. N. Zvonkov, J. Phys. D **41**, 245110 (2008).

[30] R. Danneau, O. Klochan, W. R. Clarke, L. H. Ho, A. P. Micolich, M. Y. Simmons, A. R. Hamilton, M. Pepper, D. A. Ritchie, and U. Zulicke, Phys. Rev. Lett. **97**, 026403 (2006).

[31] R. E. Miles, P. Harrison, and D. Lippens, *Terahertz Sources and Systems* (Kluwer Academic, Dordrecht, 2001), NATO Science Series, Ser. II, Vol. 27.

[32] A. Deninger and T. Renner, Laser Focus World **44**, 111 (2008).

[33] M. Sherwin, Nature (London) **420**, 131 (2002).

[34] G. L. Carr, M. C. Martin, W. R. McKinney, K. Jordan, G. R. Neil, and G. P. Williams, Nature (London) **420**, 153 (2002).

[35] M. C. Hoffmann, J. Hebling, H. Y. Hwang, K.-L. Yeh, and K. A. Nelson, J. Opt. Soc. Am. B **26**, A29 (2009).

[36] S. K. Singh, B. D. McCombe, J. Kono, S. J. Allen, I. Lo, W. C. Mitchel, and C. E. Stutz, Phys. Rev. B **58**, 7286 (1998).

[37] S. Yamada, Science and Technology of Advanced Materials **6**, 406 (2005).

[38] T. Sugaya, J. P. Bird, D. K. Ferry, A. Sergeev, V. Mitin, K.-Y. Jang, M. Ogura, and Y. Sugiyama, Appl. Phys. Lett. **81**, 727 (2002).